Published in final edited form as:
Behav Brain Res. 2014 May 15; 265: 171–180. doi:10.1016/j.bbr.2014.02.033.

Bone Marrow Mononuclear Cell Transplantation Promotes Therapeutic Angiogenesis via Upregulation of the VEGF-VEGFR2 Signaling Pathway in a Rat Model of Vascular Dementia

Jianping Wang[a,*], **Xiaojie Fu**[a], **Chao Jiang**[a,b], **Lie Yu**[a], **Menghan Wang**[a], **Wei Han**[a], **Liu Liu**[a], and **Jian Wang**[b,*]

[a]Department of Neurology, The Fifth Affiliated Hospital of Zhengzhou University, Zhengzhou 450052, Henan, China

[b]Department of Anesthesiology/Critical Care Medicine, Johns Hopkins University, School of Medicine, Baltimore, MD, USA

Abstract

Bone marrow mononuclear cells (BMMNCs) are important for angiogenesis after stroke. We investigated the effects of BMMNCs on cognitive function, angiogenesis, and the vascular endothelial growth factor (VEGF)-VEGF receptor 2 (VEGFR2) signaling pathway in a rat model of vascular dementia. We transplanted BMMNCs into rats that had undergone permanent bilateral occlusion of the common carotid arteries (2VO) and observed their migration in vivo. On day 28, we assessed cognitive function with the Morris Water Maze test and examined vascular density and white matter damage within the corpus striatum by staining with fluorescein lycopersicon esculentum (tomato) lectin or Luxol fast blue. We evaluated expression of VEGF, rapidly accelerated fibrosarcoma 1 (Raf1), and extracellular-signal-regulated kinases 1 and 2 (ERK1/2) in the ischemic hemisphere by Western blot analysis on day 7 after cell transplantation. Contribution of the VEGF-VEGFR2 signaling pathway was confirmed by using VEGFR2 inhibitor SU5416. BMMNCs penetrated the blood-brain barrier and reached the ischemic cortex and white matter or incorporated into vascular walls of 2VO rats. BMMNC-treated 2VO rats had better learning and memory, higher vascular density, and less white matter damage than did vehicle-treated rats. The beneficial effects of BMMNCs were abolished by pretreatment of rats with SU5416. Protein expression of VEGF and phosphorylated Raf1 and ERK1/2 was also significantly increased by BMMNC treatment, but this upregulation was reversed by SU5416. BMMNCs can enhance angiogenesis, reduce white matter damage, and promote cognitive recovery in 2VO rats. The angiogenic effect may result from upregulation of the VEGF-VEGFR2 signaling pathway.

*Address correspondence to: Jianping Wang, MD, PhD, Department of Neurology, The Fifth Affiliated Hospital of Zhengzhou University, Zhengzhou 450052, Henan, China (Phone: 011-86-371-68322417; Fax: 86-371-66965783; wjpwfy666@126.com). Or: Jian Wang, MD, PhD, Department of Anesthesiology and Critical Care Medicine, Johns Hopkins University, School of Medicine, Baltimore, MD, USA (Phone: 443-287-5490; Fax: 410-502-5177; jwang79@jhmi.edu).

Keywords

angiogenesis; bone marrow mononuclear cells; cell transplantation; vascular dementia; VEGF-VEGFR2 signaling pathway

1. Introduction

Vascular dementia (VD) is the second most common cause of dementia after Alzheimer's disease and accounts for approximately 20% of dementia in China [1]. Chronic cerebral hypoperfusion is a major contributor to the memory dysfunction seen in patients with VD [2]. By increasing the number of functional blood vessels, therapeutic angiogenesis may reduce the extent of ischemia and improve cognition in these patients [3].

Stem-cell-based therapy has been proposed as a potential treatment for neurodegenerative diseases [4–6]. Bone marrow mononuclear cells (BMMNCs) are particularly attractive for such therapy because they are composed of different kinds of stem cells, can be rapidly isolated without cultivation, and can be used in autologous applications [7]. BMMNCs comprise mesenchymal stem cells, hematopoietic progenitor cells, endothelial progenitor cells, and more committed cell lineages [8]. Several independent groups have demonstrated that BMMNC transplantation significantly reduces ischemic impairments and increases vascular density and blood flow in ischemic disorders such as cardiovascular disease [9, 10], peripheral arterial disease [11], and diabetic foot [12].

The mechanism behind the angiogenic capacity of BMMNCs has not yet been defined. A recent study revealed that nitric oxide synthase, which is induced by vascular endothelial growth factor (VEGF), contributes to the angiogenesis that follows BMMNC transplantation in a rat model of VD [13]. VEGF plays an important role in vascular remodeling. Of its three main receptor subtypes, VEGF receptor-2 (VEGFR2) mediates most of the downstream angiogenic effects of VEGF, including microvascular permeability and endothelial cell proliferation, migration, and survival [14]. VEGFR2 triggers these events by activating intracellular tyrosine kinases of endothelial cells and multiple downstream signals, such as rapidly accelerated fibrosarcoma 1 (Raf1) [15] and extracellular-signal-regulated kinases 1 and 2 (ERK1/2) [16]. Whether BMMNCs can promote angiogenesis by upregulating the VEGF-VEGFR2 signaling pathway after VD is still unknown.

Several animal models of chronic cerebral hypoperfusion have been developed to mimic the pathological condition of clinical VD and explore the underlying mechanisms. Of these, the most-used model is bilateral carotid artery occlusion (2-vessel occlusion, 2VO) in rats [17]. Unlike other experimental animals (such as gerbil), rats have a complete circle of Willis that connects the carotid and vertebral systems. After the 2VO procedure, the circle of Willis in rats provides compensatory blood flow from the vertebral arteries to the regions that would normally be supplied by the ligated carotid arteries. Consequently, the 2VO procedure in rat causes global cerebral hypoperfusion rather than stroke [18]. In contrast to rats that undergo middle cerebral artery occlusion (MCAO), the most commonly used animal model of ischemic stroke [19], 2VO rats develop a diffuse brain lesion characterized by demyelination in the white matter [20] and cell loss in the hippocampal CA1 area. This injury impairs cognitive functions [21] without causing major motor deficits [17, 22].

Although previous reports have indicated that BMMNC treatment is effective and safe for patients with acute ischemic stroke [23], no study has examined the angiogenic effects and possible therapeutic mechanism of BMMNCs in VD. We hypothesized that BMMNCs would improve functional outcome and promote therapeutic angiogenesis by upregulating the VEGF-VEGFR2 signaling pathway in a rat model of VD.

2. Materials and methods

2.1. Animals and ethics statement

Adult, male Sprague-Dawley rats (11–12 weeks old, 260–300 g) were purchased from the Animal Experimental Center of Zhengzhou University. They were housed in plastic cages (5 per cage) with free access to food and water and were maintained on a 12-h light/dark cycle at a constant temperature of 22±1°C. All protocols were approved by the Animal Care and Use Committee of Zhengzhou University. All efforts were made to minimize the number of animals used and their suffering.

2.2. Vascular dementia model

Rats were subjected to a previously reported 2VO model of VD in which the right and left common carotid arteries (CCAs) are permanently occluded [24][25]. Briefly, we anesthetized rats by intraperitoneal injection with 10% chloral hydrate (400 mg/kg) and made a midline incision in the ventral side of the neck to expose the CCAs. We gently separated the arteries from their sheaths and adjacent vagus nerves and then permanently occluded them with 5-0 silk suture under a surgical microscope. The neck wound was sutured closed and topical lidocaine applied. Successful 2VO was defined as an approximately 70% decrease in central blood flow, which was confirmed by laser-Doppler flowmetry [26]. Additionally, 55 sham-operated controls (sham) underwent the same surgical procedures but without carotid artery ligation.

2.3. Preparation of BMMNCs

Fresh BMMNCs were collected from femurs and tibias of male Sprague-Dawley rats (200–250 g; n=94) and purified by Percoll gradient centrifugation as previously reported [27]. The rats were anesthetized by an overdose of chloral hydrate and then sacrificed. Right and left femurs and tibias were aseptically dissected and cut at both ends. Bone marrow was extruded with serum-free Dulbecco’s modified Eagle’s medium (DMEM/F12; HyClone, Logan, UT). The extracted bone marrow was subjected to density-gradient centrifugation (160*g*, 25 min) in 1.083 g/mL Histopaque 1083 (Sigma-Aldrich, St. Louis, MO). The mononuclear cell layer was recovered from the gradient interface and washed three times by suspension in DMEM/F12 followed by 5-min centrifugation. The concentration of the cells was verified in a Neubauer counting chamber, and the number of viable cells was determined by trypan blue exclusion. To determine their migratory ability, we labeled a portion of the BMMNCs with bromodeoxyuridine (BrdU) by incubating them in culture medium containing 12 μg/mL BrdU (Sigma-Aldrich) for 24 h [28]. We assessed the purity of the isolated bone marrow cells as putative BMMNCs [29] by using fluorescence-activated cell sorting to determine the expression of various immunophenotypic markers. Ten million cells per rat (*n*=5) were incubated at 4°C for 30 min in phosphate-buffered saline (PBS) containing 2% fetal bovine serum and 1 μL of monoclonal antibody specific for CD34 (Santa Cruz Biotechnology, Santa Cruz, CA), CD45, CD90 (BD Biosciences, San Jose, CA), and CD117 (Abcam, Cambridge, MA, USA). To confirm the labeling rate, we incubated some BrdU-treated cells with 2 M HCl for 30 min to depurinate the DNA. Cells were then washed with PBS containing 0.1% fetal bovine serum albumin and 0.2% Tween-20 and incubated with 1 μL of anti-BrdU-fluorescein isothiocyanate (BD Biosciences) for 30 min.

2.4. Treatment and groups

The animals were randomly assigned to six groups: sham-operated rats injected with DMEM (sham+vehicle, *n*=29), sham-operated rats injected with BMMNCs (sham +BMMNC, *n*=24), 2VO rats injected with DMEM (2VO+vehicle, *n*=32), 2VO rats injected with BMMNCs (2VO+BMMNC, *n*=32), 2VO rats pretreated with VEGFR2 inhibitor SU5416 and injected with BMMNCs (2VO+SU5416+BMMNC, *n*=32), 2VO rats treated with SU5416 (2VO+SU5416, *n*=32). In addition, we administered BrdU-labeled BMMNCs to a subgroup of 2VO rats (2VO+BrdU-labeled BMMNC, *n*=15) to study the migration of BMMNCs.

Rats in the cell-treated groups were administered 3×10^{6} viable BMMNCs diluted in 300 μL of DMEM via tail vein infusion on day 4 after CCA occlusion because cerebral blood flow most resembles that of humans with VD at this time point [18]. This dose of cells was chosen because we and others have shown that systemic treatment with 1×10^{7} cells/kg (3×10^{6} cells per rat in this study) effectively promotes recovery in a rat ischemic stroke model [28, 30]. Vehicle-treated rats were infused with an equivalent volume of DMEM. SU5416-treated rats received 10 mg/kg VEGFR2 inhibitor SU5416 (Sigma-Aldrich) in DMEM by intraperitoneal injection immediately before the administration of BMMNCs. The mortality of each group was recorded. Body weights were measured weekly through day 28 after treatment and are expressed as percent change as follows: (body weight at each time point – body weight before surgery)/body weight before surgery×100% [31].

2.5. BMMNC migration

We sacrificed rats in the 2VO+BrdU-labeled BMMNC group on days 1, 3, 7, and 14 after cell transplantation to assess BMMNC migration (*n*=3 per time point). Rats were deeply anesthetized with an intraperitoneal injection of 10% chloral hydrate (400 mg/kg) and transcardially perfused with 0.01 mol/L PBS followed by 4% paraformaldehyde in 0.1 mol/L phosphate buffer (pH 7.4). Brains were removed and post-fixed in 4% paraformaldehyde overnight at 4°C, stored in a 30% sucrose/0.01 mol/L PBS solution until the tissue sank, and then cut into 20 μm coronal sections by cryoultramicrotomy (CM1100, Leica Biosystems, Germany). Finally, the free-floating sections were stored in 0.01 mol/L PBS for immunofluorescence analysis of BrdU-labeled cells according to the protocol from Abcam (Abcam, Cambridge, MA, USA). Sections were washed in 0.1 mol/L PBS (pH 7.4) with 1% Triton X-100 and then incubated in 1 mol/L HCl on ice for 10 min to break open

NIH-PA Author Manuscript

NIH-PA Author Manuscript

the DNA structure of the labeled cells. Next, sections were incubated in 2 mol/L HCl for 10 min at room temperature and then for 20 min at 37°C. Immediately after the acid washes, 0.1 mol/L borate buffer was added for 12 min at room temperature. Sections were blocked for 1 h in 0.1 mol/L PBS (pH 7.4) with 1% Triton X-100, 1 mol/L glycine, and 5% normal goat serum before being incubated overnight with anti-BrdU antibody (1:200; Santa Cruz Biotechnology). The sections were then washed in 0.1 mol/L PBS (pH 7.4) with 1% Trition X-100 and incubated for 2 h with CFL555-conjugated secondary antibody (1:500; Santa Cruz Biotechnology). Finally, the sections were rinsed in 0.01 mol/L PBS. Sections were placed on slides, and cover slips were applied with Vectashield (Vector Laboratories, Burlingame, CA). In addition, we incubated sections obtained on day 14 with a combination of primary antibodies, fluorescein lycopersicon esculentum (tomato) lectin (1:1000; Vector Laboratories), and anti-BrdU (1:200; Santa Cruz) to determine the proximity between the transplanted BMMNCs and vasculature. The stained cells and vasculature were observed under a fluorescence microscope (Olympus CKX41, Olympus, Japan), and images were captured with a digital camera (Olympus, Japan).

2.6. Histologic evaluation

Five rats each from the vehicle-treated sham group, vehicle-treated 2VO group, and BMMNC-treated 2VO group were randomly chosen for histologic evaluation of the brain 7 days after treatment. Serial sections of the dorsal hippocampal area (20 μm; bregma, −2.8 to −3.2 mm; sections internal, 50 μm) were cut with a microtome. For quantification analysis, three sections per rat with similar proximity to the bregma were chosen and stained with Cresyl violet or Fluoro-Jade B (FJB; Histo-Chem, Inc., Jefferson, AR) [32, 33].

2.6.1. Cresyl violet staining—The sections were processed with 1% Cresyl violet and dehydrated; cover slips were applied with Entellan (Millipore, Billerica, MA). The neuronal damage in the CA1 area of the hippocampus was observed in stained sections under a light microscope [34]. The nucleus and nucleic acids appeared violet, and neurons were faintly blue. We excluded neurons that appeared to be in the late stages of degeneration, as evidenced by shrunken morphology and dark staining [34]. Using 400X magnification, we averaged the number of viable neurons in three randomly chosen sections from the CA1 region of the dorsal hippocampus. Viable neurons in the vehicle-treated and BMMNC-treated 2VO groups were expressed as a percentage of the number in the sham group.

2.6.2. Fluoro-Jade B staining—FJB is commonly used for selectively staining degenerating neurons [32, 33]. All stained sections were mounted and observed under a fluorescence microscope (ZEISS ScopeA1, ZEISS, Germany) at an excitation wavelength of 450–490 nm. An investigator blind to treatment group counted FJB-positive cells at 400X magnification in three randomly selected sections from the CA1 region of the dorsal hippocampus. Cell counts are expressed as cells per 400X magnification.

2.7. Morris Water Maze

Twelve rats from each group were tested for spatial memory in the Morris Water Maze on day 28 as previously described [35]. An SLY-WMS water maze automatic control recorder (Beijing Sunny Instruments Co. Ltd, Beijing, China) was used in this experiment. The maze consisted of a black circular pool (150 cm in diameter, 50 cm high) filled with water (23–24°C, 28 cm in depth). The escape platform (12 cm in diameter) was placed 2 cm below the surface of the water and was fixed in the middle of the northeast quadrant.

2.7.1. Reference memory protocol—Rats received five training sessions (one session/day) that each consisted of three trials 15 min apart. A rat was placed in the pool and released facing the side wall at one of three starting positions chosen at random and not repeated. The rat was allowed to swim until it found the platform. If it did not succeed within 120 s, it was guided to the platform, where it was allowed to stay for 10 s, and the escape latency was recorded as 120 s. Rats were dried and returned to their cages after each trial. The mean escape latency and swimming speed of daily trials was recorded [35].

2.7.2. Probe trial—The probe trial consisted of one 2-min trial with the platform removed. The time the rat spent swimming in the northeast quadrant where the platform had been, the number of annulus crossings, and swimming speed were recorded. Videos were subsequently placed in randomized order to be scored by a trained observer blind to the experimental condition [35].

2.8. Vascular density analysis

We sacrificed six rats in each group on day 28 after treatment with BMMNCs or vehicle. Twenty-micrometer coronal brain sections that included the corpus striatum area (bregma, −0.8 to 0.2 mm; sections internal, 200 μm) were prepared for immunofluorescence staining as described previously [36, 37]. First, sections were incubated in 4% H_2O_2/methanol for 20 min to block endogenous peroxidase activity. Then they were washed in 0.1 mol/L Tris buffer (pH 7.4) and incubated overnight with fluorescein lycopersicon esculentum (tomato) lectin (1:1000; Vector Laboratories) at 4°C. Sections were rinsed three times at 4°C in 0.01 mol/L PBS for 5 min each and placed on slides. Cover slips were applied with Vectashield (Vector Laboratories). The stained vasculature was observed under a fluorescence microscope and images captured with a digital camera. We examined three different sections per rat that were approximately equidistant from the bregma in each of the six groups. For each section, at least four randomly distributed fields within the corpus striatum area (approximately 1.0–1.5 mm lateral from the midline and 4.0–4.5 mm from the cortex) were imaged for statistical analysis. A lectin-positive vessel separated from adjacent vessels was counted as one vessel. The number of these vessels was added to the number of vascular branch points (number of vessel bifurcations) to yield the total number of vessels. An investigator blinded to group quantified vascular density manually. Results are expressed as the mean number of stained vessels per 0.1 mm^2.

2.9. White matter damage

The rats used for analysis of vascular density were also used for white matter damage assessment. We stained brain sections with Luxol fast blue (LFB) to evaluate the amount of myelin in white matter, as previously reported [38] [39]. Three different sections per rat were analyzed under light microscopy at the same exposure level. At least three randomly distributed, white-matter fields from the middle of the corpus callosum and the corpus striatum were captured for each section. The areas covered by the LFB stain were quantified with ImageJ software (NIH) and expressed as a percentage of the total area of the white matter examined [39]. An average value was determined for each rat.

2.10. Western blot analysis

Six rats from each group were deeply anesthetized and decapitated on day 7 after treatment. The corpus striatum was dissected out, homogenized in radioimmunoprecipitation assay (RIPA) lysis buffer containing protease/phosphatase inhibitor mixture (Beyotime Institute of Biotechnology, China), and clarified by centrifugation (14000*g*, 20 min, 4°C). Supernatants were harvested, and protein concentrations were measured by the bicinchoninic acid assay (BCA, Beyotime Institute of Biotechnology). Samples were separated by 12% sodium dodecyl sulfate-polyacrylamide gel electrophoresis (SDS-PAGE Gel Preparation Kit, Beyotime Institute of Biotechnology) and then transferred onto polyvinylidene fluoride membranes (Millipore). Membranes were blocked for 1 h with 5% nonfat milk (Sigma-Aldrich) at 4°C and then incubated with primary antibody against VEGF (1:1000; Santa Cruz Biotechnology), Raf1 (1:300; Beijing Biosynthesis Biotechnology, Beijing, China), phosphorylated Raf1 (p-Raf1; 1:300; Beijing Biosynthesis Biotechnology), ERK1/2 (1:500; Beijing Biosynthesis Biotechnology), phosphorylated ERK1/2 (p-ERK1/2; 1:500; Beijing Biosynthesis Biotechnology), or glyceraldehyde 3-phosphate dehydrogenase (GAPDH; 1:2000; HangZhou Goodhere Biotechnology, Zhejiang, China). After three washes, membranes were incubated for 1 h at room temperature with horseradish peroxidase (HRP)-conjugated anti-rabbit IgG (1:2000; Sangon Biotech, Shanghai, China). Protein bands were visualized by enhanced chemiluminescence (Clinx Science Instruments, Shanghai, China) with an ECL Plus chemiluminescence detection kit (Beyotime Institute of Biotechnology). Optical density of the protein bands was quantified by Gel Analysis V 2.02 software (Clinx Science Instruments).

2.11. Statistical analysis

Statistical analysis was carried out with SPSS version 13.0. Results are expressed as mean ± SD. Fisher's exact test was used to examine differences in mortality among the six groups. We used one-way ANOVA followed by the least significant difference (LSD) test to analyze differences in vascular density; average LFB staining; expression of VEGF, Raf1, p-Raf1, ERK1/2, p-ERK1/2; and performance in the probe trial protocol. Repeated measures ANOVA followed by the LSD test was used to determine changes in reference memory protocol performance and differences in body weight between groups. $p<0.05$ was considered statistically significant.

3. Results

3.1. Mortality rates, body weight, and histologic changes

Fifty-two of 200 2VO rats (26%) died before cell transplantation. The mortality rates after cell/vehicle injection were 0/29 (0%) in the sham+vehicle group, 0/24 (0%) in the sham +BMMNC group, 3/32 (9.4%) in the 2VO+vehicle group, 2/32 (6.3%) in the 2VO +BMMNC group, 8/32 (25%) in the 2VO+SU5416+BMMNC group, and 6/32 (18.8%) in the 2VO+SU5416 group. Mortality rate was not significantly different among the last four groups ($p>0.05$). Compared with the sham groups, vehicle-treated 2VO rats showed focal histologic changes such as neuronal loss and degeneration in the CA1 subfield of the hippocampus on day 7 post-treatment. Such neuronal loss was reduced by transplantation of BMMNCs (Fig. 1A–D). Quantification showed that more viable neurons and fewer FJB-positive neurons were present in the CA1 region of the 2VO+BMMNC group than in that of the 2VO+vehicle group (p<0.05; Fig. 1E, F). The body weight of 2VO rats decreased rapidly before treatment. The body weight of BMMNC-treated 2VO rats recovered to an upper baseline level at 3 weeks after cell infusion, whereas that of vehicle−, BMMNC +SU5416−, and SU5416-treated 2VO rats did not recover to baseline until 4 weeks. However, the difference among the four 2VO groups was not statistically significant (p>0.05; Fig. 1G).

3.2. Characterization and migration of BMMNCs

The BMMNCs were composed of a variety of cell populations that were positive for the following phenotypic markers (mean ± SD; n=5 rats): CD 34 (15.1±1.3%), CD45 (83.2±1.1%), CD90 (10.5±0.72%), and CD117 (13.5±2.3%). The BrdU incorporation assays showed that 67.5±5.8% of cells were BrdU-positive. BrdU-labeled BMMNCs could be detected in the ischemic cortex and white matter (corpus striatum) on days 1, 3, 7, and 14 after transplantation (Fig. 2A). Double immunofluorescence staining revealed that most BMMNCs were incorporated into the vasculature, and more vascular BrdU-positive cells were observed in corpus striatum (21.1±5.5) than in cortex (14.4±5.2) on day 14 after cell transplantation (p<0.05; Fig. 2B–D).

3.3. Cognitive function

Rats that underwent the 2VO procedure exhibited significant impairment in the Morris Water Maze compared to sham groups (repeated measures ANOVA, F=93.38, p<0.01). The LSD test for multiple comparisons indicated that the 2VO+BMMNC group had better performance in this task than did the 2VO+vehicle group. Infusion of SU5416 reversed the improvement, such that performance of the 2VO+BMMNC+SU5416 group was not significantly different from that of the 2VO+vehicle group. The 2VO+SU5416 group also had longer latency to find the platform than did the vehicle-treated 2VO group (Fig. 3A). There was no difference in swimming speed among the six groups (Fig. 3B).

In the probe trial, one-way ANOVA revealed that rats in the sham groups spent more time in the target zone than did rats in the 2VO groups (F=41.37, p<0.01). LSD test for multiple comparisons showed that rats in the 2VO+BMMNC group spent more time in the target zone (44.49±6.28 s) than did rats in the other three 2VO groups (vehicle: 36.92±4.92 s; SU5416+BMMNC: 38.78±4.41 s; SU5416: 30.44±5.61 s, p<0.05). Rats in the 2VO +SU5416+BMMNC group also spent more time in the target quadrant than did rats in the 2VO+SU5416 group (p<0.05; Fig. 3C). The sham groups also had more annulus crossings than did the 2VO groups (F=18.59, p<0.05). The 2VO+BMMNC group had more annulus crossings (7.17±1.8) than did the 2VO+vehicle (3.8±1.70), 2VO+SU5416+BMMNC (3.58±0.99), and 2VO+SU5416 (3.83±1.53) groups (all p<0.05). Values in the 2VO +vehicle, 2VO+SU5416+BMMNC, and 2VO+SU5416 groups were not statistically different (Fig. 3D).

3.4. Vascular density

The 2VO groups had a significantly higher vascular density in the corpus striatum than did the sham groups 28 days after transplantation (F=10.20, p<0.01). Vascular density in the BMMNC-treated 2VO rats was significantly higher than that in the vehicle-treated rats (2VO+BMMNC: 32.13±2.89/0.1 mm^2; 2VO+vehicle: 26.28±3.63/0.1 mm^2; p<0.05). The BMMNC-induced increase in vascular density was reversed by SU5416 (2VO+BMMNC +SU5416: 26.62±1.28/0.1 mm^2; p<0.05 versus 2VO+BMMNC; Fig. 4).

3.5. White matter damage

LFB staining revealed the presence of myelin in the middle part of the corpus callosum and in the corpus striatum (Fig. 5A, B) [39]. Rats that underwent 2VO had significantly less LFB staining than did the sham groups at day 28 post-treatment (corpus striatum: F=38.24, p<0.01; middle part of corpus callosum: F=37.02, p<0.01). Quantitative analysis showed that LFB staining was significantly greater in the 2VO+BMMNC group than in the other three 2VO groups (corpus striatum, BMMNC: 15.33±1.97; vehicle: 10.13±1.34; SU5416+BMMNC: 11.33±1.63; SU5416: 9.05±0.93, p<0.05; middle part of corpus callosum, BMMNC: 77.83±2.64; vehicle: 69.33±6.44; SU5416+BMMNC: 65.01±3.46; SU5416: 64.50±7.56, p<0.05). However, no significant difference was present among the 2VO+vehicle, 2VO+SU5416, and 2VO+SU5416+BMMNC groups (Fig. 5C, D, p>0.05).

3.6. Expression of VEGF, p-Raf1, Raf1, p-ERK1/2, and ERK1/2

One-way ANOVA revealed a significant difference among the six groups in the expression of VEGF in the area of corpus striatum. 2VO rats had higher VEGF expression than did the two sham groups. VEGF expression was significantly higher in the BMMNC-treated 2VO rats than in the other five groups at day 7 after treatment (F=28.64, p<0.05; Fig. 6A, B). Additionally, phosphorylation of Raf1 and ERK1/2 was greater in the 2VO rats than in the sham rats. BMMNC treatment also significantly increased phosphorylation of Raf1 and ERK1/2. The ratios of p-Raf1/total Raf1 and p-ERK/total-ERK were significantly greater in the 2VO+BMMNC group than in the other three 2VO groups (Fig. 6A, C, and D)

4. Discussion

Our results show that BMMNCs can enhance angiogenesis, reduce white matter damage, and promote cognitive recovery after 2VO in rats. Furthermore, the angiogenic efficacy may stem from upregulation of the VEGF-VEGFR2 signaling pathway. Although previous researchers have reported that BMMNC transplantation is an effective therapy for cerebral ischemia [23, 28], little research has evaluated the therapeutic effect of BMMNCs in chronic cerebral hypoperfusion or VD. To the best of our knowledge, this study is the first to explore the angiogenic mechanism of BMMNCs in a 2VO rat model.

The blood-brain barrier (BBB), which restricts molecules larger than 500 Da from reaching the central nervous system, is a barrier to many neurologic therapies, including cell transplantation [40]. Previous studies have shown that BMMNCs could not penetrate the healthy rat brain [41]; however, if the BBB is made permeable, BMMNCs can migrate to the infarct area after MCAO [13, 28, 29]. In the 2VO rat model, it has been shown that appreciable opening of the BBB occurs by 6 h after a 10-min occlusion of the CCAs [42]. Additionally, BMMNCs were shown to migrate to the ischemic brain in a modified mouse model of chronic cerebral hypoperfusion, in which the CCAs were partly occluded by a micro-coil with an inner diameter of 0.18 mm, rather than permanently occluded by ligature [13].

In our model, we show that BMMNCs can penetrate the BBB and reach the ischemic brain in 2VO rats. Because the CCAs were permanently occluded, our data also indicate that BMMNCs can reach the ischemic frontoparietal area through posterior cerebral or other collateral circulation in 2VO rats. BMMNCs are appealing as potential therapy [43] because they are a heterogeneous cell fraction composed of hematopoietic stem, progenitor, and differentiated cells; mesenchymal stem cells; and endothelial progenitor cells [7]. After cerebral ischemia, the chemokine stromal-derived factor-1 is upregulated [44], which may attract BMMNCs to adhere and migrate to the infarct area [45, 46].

Our recent research showed that BMMNCs can differentiate into smooth muscle cells and endothelial cells in a rat model of permanent MCAO [29]. As in our current results, we found that BMMNCs incorporate into vessels by day 14 after transplantation. Previously, the mechanism by which BMMNCs contribute to angiogenesis has been considered to relate mainly to chemoattraction and local paracrine action, such as release of angiogenic factors [43]. Researchers have demonstrated that mesenchymal stem cells and endothelial progenitor cells, which are components of BMMNCs, improve post-ischemic angiogenesis via paracrine activation of VEGF, thereby leading to a better outcome [47], [48]. In our study, the expression of VEGF, p-Raf1, and p-ERK; the vascular density; and LFB in corpus striatum were significantly greater in 2VO+BMMNC rats than in 2VO+vehicle rats. The results of the Morris Water Maze also showed that 2VO rats treated with BMMNCs had better learning ability than did those treated with vehicle. Taken together, the evidence indicates that BMMNCs may increase the level of VEGF as well as levels of p-Raf1 and p-ERK (downstream proteins in the VEGFR2 signaling pathway [49]), increase vascular density, reduce white matter lesions, and finally, lead to a better cognitive outcome in 2VO rats.

To support our hypothesis, we inhibited VEGFR2 with SU5416 (10 mg/kg) and observed the effects of BMMNC transplantation in the 2VO rats. It was previously shown that VEGFR2 inhibition in rats by intraperitoneal injection of SU5416 (10 mg/kg/day) for 3 days beginning the second day after MCAO does not substantially affect vessel permeability but does increase tissue injury and cell death and limit endothelial cell proliferation in the brain [50]. Similarly, we found that SU5416 did not significantly alter vascular density or the expression of VEGF, p-Raf1, or p-ERK. Neither did it cause myelin loss, which can significantly worsen performance in learning and memory tests. One study has shown that inhibition of VEGFR2 after traumatic brain injury in rats increases lesion volume and cell death [51]. These effects could explain why the 2VO+SU5416 group had worse performance than the 2VO+vehicle group in the Morris Water Maze.

Expression levels of p-Raf1 and p-ERK were lower in the 2VO+SU5416+BMMNC group than in the 2VO+BMMNC group, as was the vascular density, LFB, and Morris Water Maze performance. These differences indicate that the beneficial effects of BMMNC treatment were abrogated by inhibition of the VEGFR2 signaling pathway. Interestingly, VEGF expression was significantly lower in the 2VO+SU5416+BMMNC group than in the 2VO +BMMNC group, indicating that the inhibition of VEGFR2 also affects the ability of BMMNCs to upregulate VEGF. Research has shown that under ischemic conditions, VEGF promotes BBB permeability [52], which would facilitate migration of BMMNCs into the brain. Thus, upregulation of VEGF by BMMNCs may produce a positive feedback loop. Moreover, inhibition of VEGFR2 likely reduces the function of VEGF, thereby limiting the migration of BMMNCs into the ischemic brain.

Our study suggests that transplantation of BMMNCs increases vascular density, reduces white matter damage, and improves learning and memory in 2VO rats. The likely mechanism is via upregulation of the VEGF-VEGFR2 signaling pathway, which enhances angiogenesis. It remains to be determined what the dose-response relationship of BMMNC transplantation is and whether the therapeutic effect is also present in female rats that have undergone 2VO. In addition, further exploration is warranted to determine which constituents of BMMNCs participate in the angiogenic process.

Acknowledgments

This work was supported by grants from NSFC (81271284), The Overseas Training Program of Henan Province Medical Academic Leaders (2011023), AHA (13GRNT15730001), and NIH (K01AG031926, R01NS078026, R01AT007317). We thank Claire Levine for assistance with this manuscript.

References

1. Chan KY, Wang W, Wu JJ, et al. Epidemiology of Alzheimer's disease and other forms of dementia in China, 1990–2010: a systematic review and analysis[J]. Lancet. 2013; 381(9882):2016–2023. [PubMed: 23746902]
2. Stasiak A, Mussur M, Unzeta M, et al. The central histamine level in rat model of vascular dementia[J]. J Physiol Pharmacol. 2011; 62(5):549–558. [PubMed: 22204803]
3. Brown WR, Thore CR. Review: cerebral microvascular pathology in ageing and neurodegeneration[J]. Neuropathol Appl Neurobiol. 2011; 37(1):56–74. [PubMed: 20946471]
4. Lindvall, O.; Kokaia, Z.; Martinez-Serrano, A. Stem cell therapy for human neurodegenerative disorders--how to make it work[J]. 2004.
5. Tajiri N, Acosta S, Glover LE, et al. Intravenous grafts of amniotic fluid-derived stem cells induce endogenous cell proliferation and attenuate behavioral deficits in ischemic stroke rats[J]. PLoS One. 2012; 7(8):e43779. [PubMed: 22912905]
6. Ishikawa H, Tajiri N, Shinozuka K, et al. Vasculogenesis in experimental stroke after human cerebral endothelial cell transplantation[J]. Stroke. 2013; 44(12):3473–3481. [PubMed: 24130140]
7. Giraldi-Guimaraes A, de Freitas HT, Coelho BP, et al. Bone marrow mononuclear cells and mannose receptor expression in focal cortical ischemia[J]. Brain Res. 2012; 1452:173–184. [PubMed: 22459039]
8. Perin, EC.; Silvia, GV.; Willerson, JT. Informa Healthcare. An Essential Guide to Cardiac Cell Therapy[M]. 2006.222
9. Kim H, Cho HJ, Kim SW, et al. CD31+ cells represent highly angiogenic and vasculogenic cells in bone marrow: novel role of nonendothelial CD31+ cells in neovascularization and their therapeutic effects on ischemic vascular disease[J]. Circ Res. 2010; 107(5):602–614. [PubMed: 20634489]
10. Napoli C, Maione C, Schiano C, et al. Bone marrow cell-mediated cardiovascular repair: potential of combined therapies[J]. Trends Mol Med. 2007; 13(7):278–286. [PubMed: 17574919]

11. Raval Z, Losordo DW. Cell therapy of peripheral arterial disease: from experimental findings to clinical trials[J]. Circ Res. 2013; 112(9):1288–1302. [PubMed: 23620237]
12. Tateishi-Yuyama E, Matsubara H, Murohara T, et al. Therapeutic angiogenesis for patients with limb ischaemia by autologous transplantation of bone-marrow cells: a pilot study and a randomised controlled trial[J]. Lancet. 2002; 360(9331):427–435. [PubMed: 12241713]
13. Fujita Y, Ihara M, Ushiki T, et al. Early protective effect of bone marrow mononuclear cells against ischemic white matter damage through augmentation of cerebral blood flow[J]. Stroke. 2010; 41(12):2938–2943. [PubMed: 20947840]
14. Carmeliet P, Ferreira V, Breier G, et al. Abnormal blood vessel development and lethality in embryos lacking a single VEGF allele[J]. Nature. 1996; 380(6573):435–439. [PubMed: 8602241]
15. Gollob JA, Wilhelm S, Carter C, et al. Role of Raf kinase in cancer: therapeutic potential of targeting the Raf/MEK/ERK signal transduction pathway[J]. Semin Oncol. 2006; 33(4):392–406. [PubMed: 16890795]
16. Narasimhan P, Liu J, Song YS, et al. VEGF Stimulates the ERK 1/2 signaling pathway and apoptosis in cerebral endothelial cells after ischemic conditions[J]. Stroke. 2009; 40(4):1467–1473. [PubMed: 19228841]
17. Jiwa NS, Garrard P, Hainsworth AH. Experimental models of vascular dementia and vascular cognitive impairment: a systematic review[J]. J Neurochem. 2010; 115(4):814–828. [PubMed: 20731763]
18. Farkas E, Luiten PG, Bari F. Permanent, bilateral common carotid artery occlusion in the rat: a model for chronic cerebral hypoperfusion-related neurodegenerative diseases[J]. Brain Res Rev. 2007; 54(1):162–180. [PubMed: 17296232]
19. Sicard KM, Fisher M. Animal models of focal brain ischemia[J]. Exp Transl Stroke Med. 2009; 1:7. [PubMed: 20150985]
20. Wakita H, Tomimoto H, Akiguchi I, et al. Ibudilast, a phosphodiesterase inhibitor, protects against white matter damage under chronic cerebral hypoperfusion in the rat[J]. Brain Res. 2003; 992(1): 53–59. [PubMed: 14604772]
21. Vicente E, Degerone D, Bohn L, et al. Astroglial and cognitive effects of chronic cerebral hypoperfusion in the rat[J]. Brain Res. 2009; 1251:204–212. [PubMed: 19056357]
22. Huang J, Yin SJ, Chen YJ, et al. Transplanted bone marrow stromal cells improve cognitive dysfunction due to aging hypoperfusion in rats[J]. Chin Med J (Engl). 2010; 123(24):3620–3625. [PubMed: 22166641]
23. Savitz SI, Misra V, Kasam M, et al. Intravenous autologous bone marrow mononuclear cells for ischemic stroke[J]. Ann Neurol. 2011; 70(1):59–69. [PubMed: 21786299]
24. Ganzella M, de Oliveira ED, Comassetto DD, et al. Effects of chronic guanosine treatment on hippocampal damage and cognitive impairment of rats submitted to chronic cerebral hypoperfusion[J]. Neurol Sci. 2012; 33(5):985–997. [PubMed: 22167652]
25. Winocur G, Thompson C, Hakim A, et al. The effects of high- and low-risk environments on cognitive function in rats following 2-vessel occlusion of the carotid arteries: A behavioral study[J]. Behav Brain Res. 2013
26. Choy M, Ganesan V, Thomas DL, et al. The chronic vascular and haemodynamic response after permanent bilateral common carotid occlusion in newborn and adult rats[J]. J Cereb Blood Flow Metab. 2006; 26(8):1066–1075. [PubMed: 16395291]
27. Fukushima S, Varela-Carver A, Coppen SR, et al. Direct intramyocardial but not intracoronary injection of bone marrow cells induces ventricular arrhythmias in a rat chronic ischemic heart failure model[J]. Circulation. 2007; 115(17):2254–2261. [PubMed: 17438152]
28. Jiang C, Wang J, Yu L, et al. Comparison of the therapeutic effects of bone marrow mononuclear cells and microglia for permanent cerebral ischemia[J]. Behav Brain Res. 2013; 250C:222–229. [PubMed: 23685323]
29. Wang J, Yu L, Jiang C, et al. Bone marrow mononuclear cells exert long-term neuroprotection in a rat model of ischemic stroke by promoting arteriogenesis and angiogenesis[J]. Brain Behav Immun. 2013

30. Yang B, Strong R, Sharma S, et al. Therapeutic time window and dose response of autologous bone marrow mononuclear cells for ischemic stroke[J]. J Neurosci Res. 2011; 89(6):833–839. [PubMed: 21412816]
31. Wu H, Wu T, Xu X, et al. Iron toxicity in mice with collagenase-induced intracerebral hemorrhage[J]. J Cereb Blood Flow Metab. 2011; 31(5):1243–1250. [PubMed: 21102602]
32. Wang J, Fields J, Zhao C, et al. Role of Nrf2 in protection against intracerebral hemorrhage injury in mice[J]. Free Radic Biol Med. 2007; 43(3):408–414. [PubMed: 17602956]
33. Wang J, Tsirka SE. Tuftsin fragment 1–3 is beneficial when delivered after the induction of intracerebral hemorrhage[J]. Stroke. 2005; 36(3):613–618. [PubMed: 15692122]
34. Yeganeh F, Nikbakht F, Bahmanpour S, et al. Neuroprotective effects of NMDA and group I metabotropic glutamate receptor antagonists against neurodegeneration induced by homocysteine in rat hippocampus: in vivo study[J]. J Mol Neurosci. 2013; 50(3):551–557. [PubMed: 23564299]
35. Cechetti F, Worm PV, Pereira LO, et al. The modified 2VO ischemia protocol causes cognitive impairment similar to that induced by the standard method, but with a better survival rate[J]. Braz J Med Biol Res. 2010; 43(12):1178–1183. [PubMed: 21085899]
36. Bengoetxea H, Argandona EG, Lafuente JV. Effects of visual experience on vascular endothelial growth factor expression during the postnatal development of the rat visual cortex[J]. Cereb Cortex. 2008; 18(7):1630–1639. [PubMed: 17986606]
37. Wang J, Dore S. Heme oxygenase-1 exacerbates early brain injury after intracerebral haemorrhage[J]. Brain. 2007; 130(Pt 6):1643–1652. [PubMed: 17525142]
38. Wu H, Wu T, Li M, et al. Efficacy of the lipid-soluble iron chelator 2, 2′-dipyridyl against hemorrhagic brain injury[J]. Neurobiol Dis. 2012; 45(1):388–394. [PubMed: 21930208]
39. Paris D, Beaulieu-Abdelahad D, Mullan M, et al. Amelioration of experimental autoimmune encephalomyelitis by anatabine[J]. PLoS One. 2013; 8(1):e55392. [PubMed: 23383175]
40. Bleier BS, Kohman RE, Feldman RE, et al. Permeabilization of the Blood-Brain Barrier via Mucosal Engrafting: Implications for Drug Delivery to the Brain[J]. PLoS One. 2013; 8(4):e61694. [PubMed: 23637885]
41. Brenneman M, Sharma S, Harting M, et al. Autologous bone marrow mononuclear cells enhance recovery after acute ischemic stroke in young and middle-aged rats[J]. J Cereb Blood Flow Metab. 2010; 30(1):140–149. [PubMed: 19773802]
42. Preston E, Foster DO. Evidence for pore-like opening of the blood-brain barrier following forebrain ischemia in rats[J]. Brain Res. 1997; 761(1):4–10. [PubMed: 9247060]
43. Mendez-Otero R, de Freitas GR, Andre C, et al. Potential roles of bone marrow stem cells in stroke therapy[J]. Regen Med. 2007; 2(4):417–423. [PubMed: 17635049]
44. Hill WD, Hess DC, Martin-Studdard A, et al. SDF-1 (CXCL12) is upregulated in the ischemic penumbra following stroke: association with bone marrow cell homing to injury[J]. J Neuropathol Exp Neurol. 2004; 63(1):84–96. [PubMed: 14748564]
45. Stumm RK, Rummel J, Junker V, et al. A dual role for the SDF-1/CXCR4 chemokine receptor system in adult brain: isoform-selective regulation of SDF-1 expression modulates CXCR4-dependent neuronal plasticity and cerebral leukocyte recruitment after focal ischemia[J]. J Neurosci. 2002; 22(14):5865–5878. [PubMed: 12122049]
46. Borlongan CV, Glover LE, Tajiri N, et al. The great migration of bone marrow-derived stem cells toward the ischemic brain: therapeutic implications for stroke and other neurological disorders[J]. Prog Neurobiol. 2011; 95(2):213–228. [PubMed: 21903148]
47. Katare R, Riu F, Rowlinson J, et al. Perivascular Delivery of Encapsulated Mesenchymal Stem Cells Improves Postischemic Angiogenesis Via Paracrine Activation of VEGF-A[J]. Arterioscler Thromb Vasc Biol. 2013
48. Alev C, Ii M, Asahara T. Endothelial progenitor cells: a novel tool for the therapy of ischemic diseases[J]. Antioxid Redox Signal. 2011; 15(4):949–965. [PubMed: 21254837]
49. Novo E, Cannito S, Zamara E, et al. Proangiogenic cytokines as hypoxia-dependent factors stimulating migration of human hepatic stellate cells[J]. Am J Pathol. 2007; 170(6):1942–1953. [PubMed: 17525262]

50. Shimotake J, Derugin N, Wendland M, et al. Vascular endothelial growth factor receptor-2 inhibition promotes cell death and limits endothelial cell proliferation in a neonatal rodent model of stroke[J]. Stroke. 2010; 41(2):343–349. [PubMed: 20101028]

51. Skold MK, Risling M, Holmin S. Inhibition of vascular endothelial growth factor receptor 2 activity in experimental brain contusions aggravates injury outcome and leads to early increased neuronal and glial degeneration[J]. Eur J Neurosci. 2006; 23(1):21–34. [PubMed: 16420412]

52. Zhang ZG, Zhang L, Jiang Q, et al. VEGF enhances angiogenesis and promotes blood-brain barrier leakage in the ischemic brain[J]. J Clin Invest. 2000; 106(7):829–838. [PubMed: 11018070]

NIH-PA Author Manuscript

NIH-PA Author Manuscript

Highlights

- We treated 2VO rats with bone marrow mononuclear cells (BMMNCs).
- BMMNC transplantation promoted therapeutic angiogenesis in 2VO rats.
- The effects of BMMNCs in 2VO rats were abolished by pretreatment of SU5416.
- The angiogenic effect may result from upregulation of VEGF-VEGFR2 pathway.

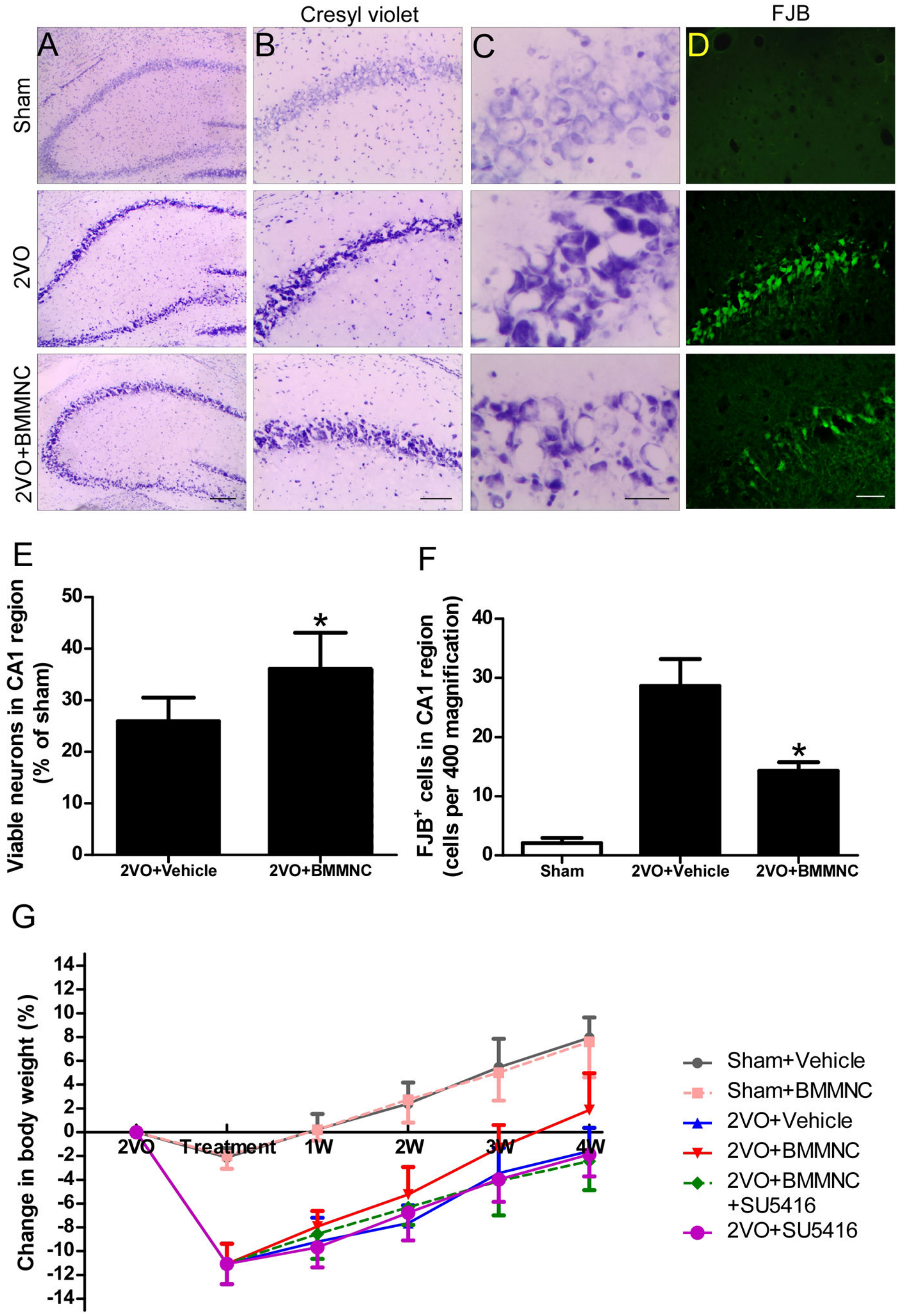

Figure 1.

BMMNC transplantation alleviates neuronal damage in the CA1 subfield of hippocampus but does not affect body weight changes. (A–D) Neuronal damage in the hippocampal CA1 region was greater in vehicle-treated 2VO rats than in vehicle-treated sham rats on day 7 post-treatment. BMMNC transplantation mitigated the neuronal loss and degeneration in the CA1 region. Scale bars: A = 200 μm, B = 100 μm, C = 20 μm, D=30 μm. *n*=5/group. (E–F) Quantification showed that more viable neurons and Fluoro-Jade B-positive neurons were present in the CA1 region of the 2VO+BMMNC group than in that of the 2VO+vehicle group. **p*<0.05 vs. vehicle-treated group. (G) Changes in rat body weight over the course of the experiment (*n*=18/group). Although BMMNC treatment promoted recovery of body weight, no significant difference was found among the four 2VO groups. *p*>0.05.

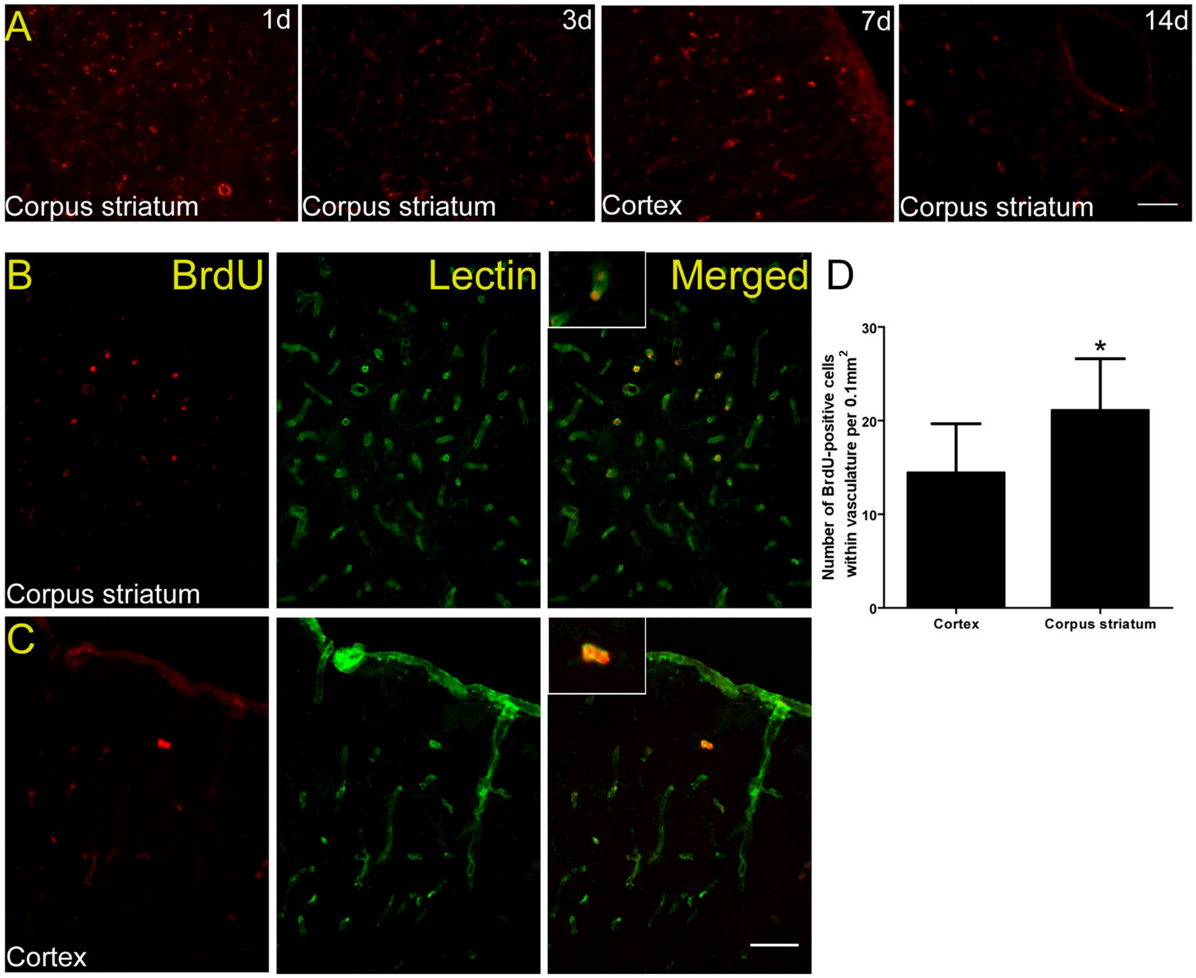

Figure 2.

In vivo migration of BMMNCs in rats that underwent 2VO. (A) Immunofluorescence staining for BrdU-labeled cells revealed that BMMNCs (red) migrated to both cortex (7 days) and white matter (corpus striatum area, 1, 3, and 14 days). (B) Double Immunofluorescence staining showed that BMMNCs (red) can be detected 2 weeks after transplantation in the area of corpus striatum. (C) The distribution of BMMNCs in the area of frontoparietal cortex. Most cells were incorporated into the vascular wall by day 14 after cell transplantation. Scale bars = 50 μm. *n*=3 at each time point. (D) Quantification showed that more vascular BrdU-positive cells were present in corpus striatum than in cortex. *$p<0.05$.

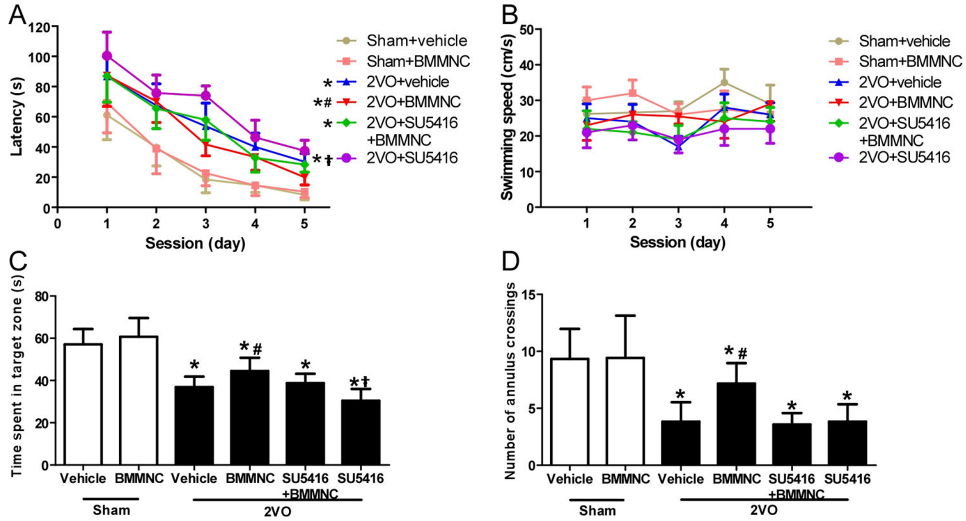

Figure 3.

BMMNCs improve learning and memory at day 28 after treatment. (A) Latency to find the platform in the Morris Water Maze test. Rats that had undergone 2VO exhibited worse performance than did the sham-operated rats. Treatment of 2VO rats with BMMNCs decreased the latency to find the platform (improved learning) compared to vehicle treatment. 2VO rats infused with SU5416 (2VO+SU5416) had poorer performance than did the 2VO+vehicle and 2VO+ SU5416+BMMNC groups. *p<0.01 vs. the sham groups; #p<0.01 vs. the other three 2VO groups; †p<0.05 vs. 2VO+vehicle group. (B) There was no difference in swimming speed among the six groups during the five sessions. (C) Quantification of time spent in the target zone during the probe trial indicated that sham groups spent more time in the correct quadrant than did the 2VO groups. The 2VO+BMMNC group exhibited better performance than did the other three 2VO groups. The 2VO+SU5416 group spent less time in the target zone than did the 2VO+SU5416+BMMNC group. *p<0.01 vs. sham groups; #p<0.05 vs. the other three 2VO groups; †p<0.05 vs. 2VO+SU5416+BMMNC group. (D) Sham groups had more crossings of the annulus than did the 2VO groups. 2VO rats treated with BMMNCs had more crossings than did vehicle-treated, SU5416+BMMNC-treated, or SU5416-treated 2VO rats. *p<0.05 vs. sham groups; #p<0.05 vs. the other three 2VO groups. n=12/group.

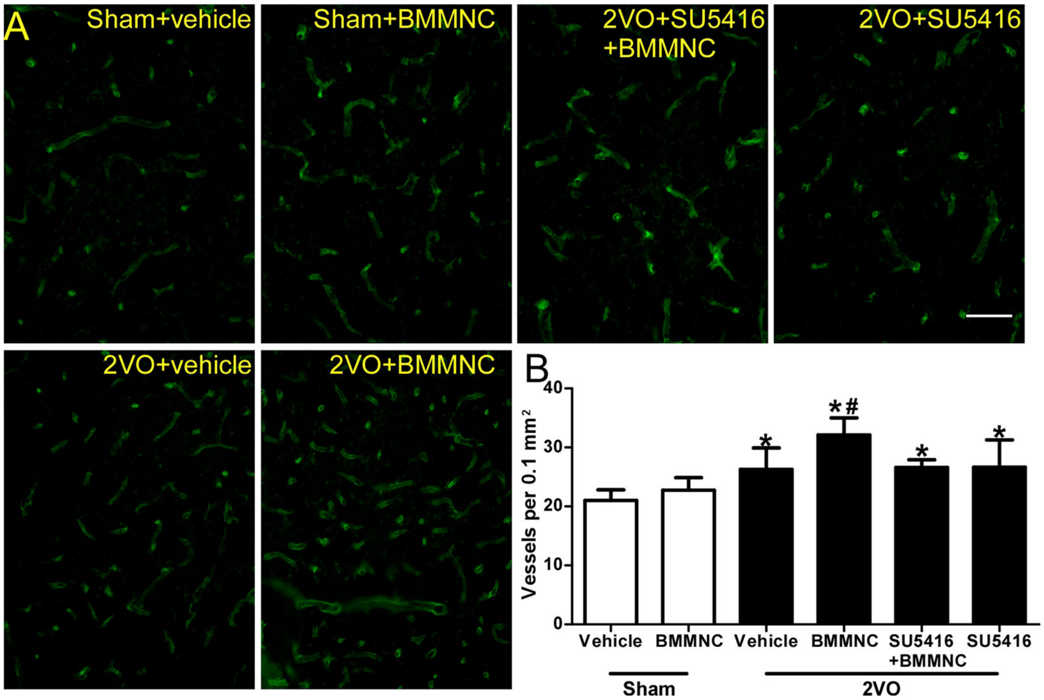

Figure 4.

BMMNCs facilitate angiogenesis in 2VO rats. (A) Immunofluorescence staining of blood vessels (green) with fluorescein lycopersicon esculentum (tomato) lectin in corpus striatum on day 28 after administration of BMMNCs. (B) Quantification showed that 2VO groups had significantly higher vascular density than did sham groups. In addition, the vascular density of the 2VO+BMMNC group was significantly higher than that of the other three 2VO groups. *p<0.01 vs. sham groups. #p<0.01 vs. the other three 2VO groups. Scale bar = 50 μm. n=6/group.

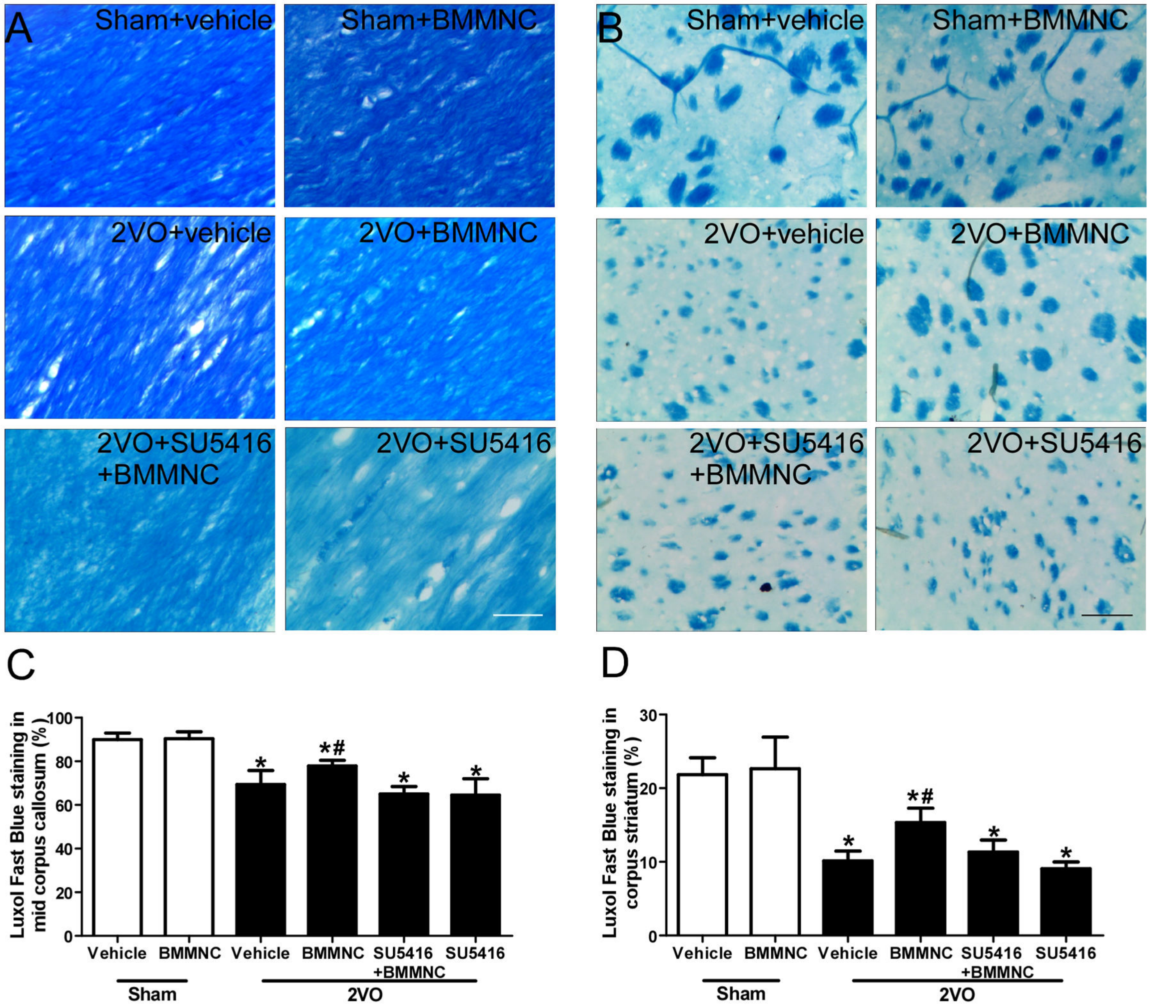

Figure 5.

BMMNCs decrease white matter lesions in mid corpus callosum and corpus striatum of rats with 2VO. (A) Luxol fast blue staining of the middle of the corpus callosum on day 28 after treatment with BMMNCs. (B) Luxol fast blue staining of the corpus striatum on day 28 after treatment with BMMNCs. Scale bars in A and B = 30 μm. (C, D) Quantification of Luxol fast blue staining of the mid corpus callosum and corpus striatum shows that 2VO rats had less myelin than did sham groups. BMMNC transplantation significantly increased Luxol fast blue staining, but the effect was neutralized by SU5416. *p<0.01 vs. sham groups. #p<0.01 vs. the other three 2VO groups. n=6/group.

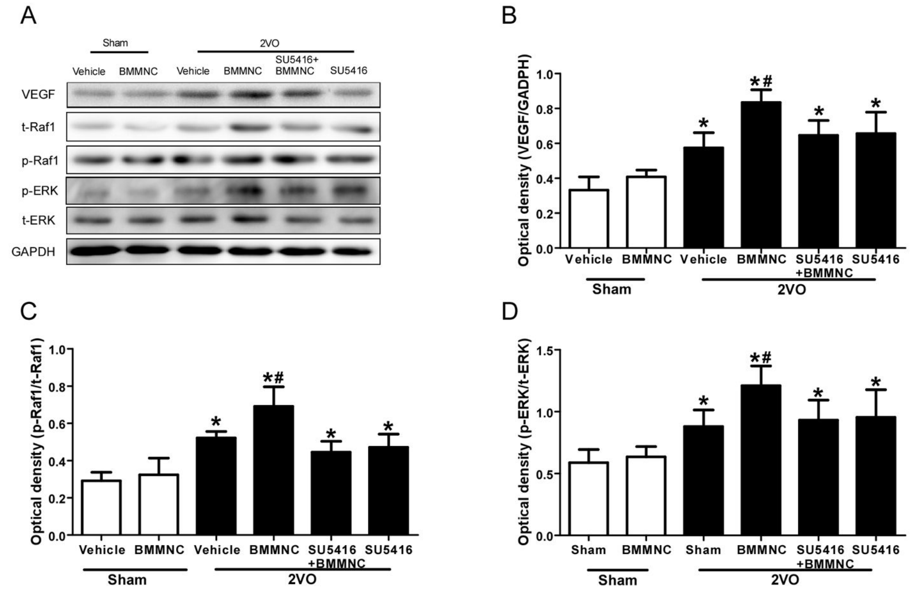

Figure 6.

BMMNCs increase the expression of VEGF, phosphorylated Raf1 (p-Raf1), and phosphorylated ERK1/2 (p-ERK) in 2VO rats. (A) Western blot analysis of VEGF, p-Raf1, total (t) Raf1, p-ERK, and t-ERK1/2 on day 7 after BMMNC transplantation. Glyceraldehyde 3-phosphate dehydrogenase (GAPDH) was used as a loading control. (B) Quantification of band densities showed that VEGF expression was significantly greater in the 2VO group treated with BMMNCs than in the other three 2VO groups. *$p<0.05$ vs. sham groups; #$p<0.05$ vs. the other three 2VO groups. (C, D) Quantification of band densities as a ratio of phosphorylated protein/total protein showed that BMMNC treatment significantly increased Raf1 and ERK1/2 phosphorylation compared to that in the two sham groups and the other three 2VO groups. *$p<0.05$ vs. sham groups; #$p<0.05$ vs. the other three 2VO groups. $n=6$ per group.